

Acta Crystallographica Section D

**Biological  
Crystallography**

ISSN 0907-4449

## Phasing at high resolution using Ta<sub>6</sub>Br<sub>12</sub> cluster

Sankaran Banumathi, Mirosława Dauter and Zbigniew Dauter

Copyright © International Union of Crystallography

Author(s) of this paper may load this reprint on their own web site provided that this cover page is retained. Republication of this article or its storage in electronic databases or the like is not permitted without prior permission in writing from the IUCr.

Phasing at high resolution using Ta<sub>6</sub>Br<sub>12</sub> clusterSankaran Banumathi,<sup>a</sup> Mirosława Dauter<sup>b</sup> and Zbigniew Dauter<sup>a\*</sup>

<sup>a</sup>Synchrotron Radiation Research Section,  
Macromolecular Crystallography Laboratory,  
NCI, Brookhaven National Laboratory,  
Building 725A-X9, Upton, NY 11973, USA, and  
<sup>b</sup>SAIC-Frederick Inc., Basic Research Program,  
Brookhaven National Laboratory,  
Building 725A-X9, Upton, NY 11973, USA

Correspondence e-mail: dauter@bnl.gov

Received 4 November 2002

Accepted 3 January 2003

The Ta<sub>6</sub>Br<sub>12</sub><sup>2+</sup> cluster compound is known to be a powerful reagent for derivatization of crystals of large macromolecules at low resolution. The cluster is a regular octahedron of six Ta atoms with 12 bridging Br atoms at the edges of the octahedron. The cluster is compact, of approximately spherical shape, with a radius of about 6 Å. Both tantalum and bromine display a significant anomalous diffraction signal at their absorption edges at 1.25 and 0.92 Å, respectively. At resolutions lower than 5 Å the tantalum cluster behaves as a super-atom and provides very large isomorphous and anomalous signals, which significantly diminish at about 4 Å. However, beyond 3 Å the individual Ta atoms can be resolved and the phasing power of the cluster increases again. The Ta<sub>6</sub>Br<sub>12</sub><sup>2+</sup> cluster has been used for phasing four different proteins at high resolution. Ta<sub>6</sub>Br<sub>12</sub><sup>2+</sup> appeared to be a mild derivatization reagent and, despite partial incorporation, led to a successful solution of crystal structures by the single-wavelength anomalous diffraction (SAD) approach.

### 1. Introduction

In the earlier period of macromolecular crystallography, the primary method of phasing new crystal structures was through the use of the isomorphous differences between the reflection intensities measured from native crystals and from crystals derivatized with heavy-atom reagents. Progress in the last decade, mainly connected with the wider availability of synchrotron beamlines, crystal-freezing techniques and improvements in data collection, processing, phasing algorithms and programs, has changed this situation to some extent. Whereas previously the anomalous scattering signal was treated as an auxiliary source of phasing, it is at present used as a primary phasing vehicle, mainly through the multi-wavelength anomalous dispersion (MAD) approach (Smith & Hendrickson, 2001). The most popular anomalous scatterer is selenium, introduced into proteins in the form of selenomethionine, but several other elements are also often used, such as Hg, Pt, Au or Br. Some attention has recently been directed to phasing based on the single-wavelength anomalous dispersion (SAD) approach (Rice *et al.*, 2000; Dauter *et al.*, 2002). For both MAD and SAD methods, it is advantageous to use elements with large anomalous scattering contributions. Among scatterers that display highly resonant white lines in their fluorescence spectra are the lanthanides and some elements close to them in the periodic table (Hendrickson & Ogata, 1997).

Tantalum has an atomic number of 73 and its *L*<sub>III</sub> X-ray absorption edge at 1.254 Å is characterized by a pronounced white line. Owing to this property, the octahedral cluster ion

**Table 1**

Diffraction data.

Values in parentheses correspond to the highest resolution shell.

| Protein                                    | Glucose isomerase   | Thaumatin   | Thermolysin  | Lysozyme                                 |
|--|---|---|--|--|
| Space group                                | <i>I</i> 222  | <i>P</i> 4 <sub>1</sub> 2 <sub>1</sub> 2                          | <i>P</i> 6 <sub>1</sub> 22   | <i>P</i> 4 <sub>3</sub> 2 <sub>1</sub> 2 |
| Unit-cell parameters (Å)                   |   |   |  |  |
| <i>a</i>                                   | 92.70   | 57.76   | 92.57  | 78.35                                    |
| <i>b</i>                                   | 97.20   | 57.76   | 92.57  | 78.35                                    |
| <i>c</i>                                   | 102.78  | 149.98  | 128.30   | 37.00                                    |
| Resolution range (Å)                       | 30–1.3 (1.35–1.30)  | 20–1.5 (1.55–1.50)  | 30–1.6 (1.66–1.60)   | 20–1.5 (1.55–1.50)                       |
| Completeness† (%)                          | 99.6 (91.2)   | 99.7 (99.6)   | 98.0 (96.7)  | 99.9 (100)                               |
| <i>R</i> <sub>merge</sub> (%)              | 5.0 (47.5)  | 4.6 (12.7)  | 3.9 (20.9)   | 6.1 (37.3)                               |
| <i>I</i> /σ( <i>I</i> )                    | 20.6 (1.7)  | 45.6 (13.4)   | 68.4 (10.5)  | 38.0 (4.7)                               |
| Multiplicity                               | 3   | 6   | 4  | 5.8                                      |
| <i>B</i> factor (Wilson) (Å <sup>2</sup> ) | 13.5  | 13.8  | 19.4   | 19.0                                     |
| <i>R</i> / <i>R</i> <sub>free</sub> (%)    | 12.2/13.8‡  | 17.2/18.8   | 18.0/20.5  | 20.6/22.0                                |
| Crystallization conditions                 | 22% MPD, 1 <i>M</i> Tris, 0.2 <i>M</i> MgCl <sub>2</sub> , pH 7.0 | 0.8 <i>M</i> K <sub>2</sub> Na tartrate, 0.1 <i>M</i> ADA, pH 6.5 | 45% DMSO, 1.4 <i>M</i> Ca(OAc) <sub>2</sub> , 1 <i>M</i> Tris pH 7.3 | 10% NaCl, 0.2 <i>M</i> NaOAc, pH 4.7     |
| Cryo-soaking conditions                    | 30% MPD added   | 25% glycerol added  | 15% glycerol added   | 30% glycerol added                       |

† The completeness relates to the individual Friedel mates. ‡ This model was refined anisotropically with *SHELXL*.

Ta<sub>6</sub>Br<sub>12</sub><sup>2+</sup> has been introduced as a powerful derivatization reagent for phasing macromolecular crystal structures (Schneider & Lindqvist, 1994; Knäblein *et al.*, 1997). So far, it has been mostly used for phasing large crystal structures of proteins and complexes at low resolution (Lindqvist *et al.*, 1992; Schneider *et al.*, 1996; Thygesen *et al.*, 1996; Ban *et al.*, 2000; Gomis-Rüth & Coll, 2001). Indeed, at resolutions lower than 5 Å the cluster scatters as a super-atom, which enhances its isomorphous and anomalous diffraction signals. At intermediate resolutions, around 4.5–3.5 Å, these signals diminish considerably. However, beyond 3.0 Å resolution the individual Ta atoms located in the cluster at mutual distances of 2.7 Å can be resolved and the signal of the Ta atoms increases again. The scattering behavior of Ta<sub>6</sub>Br<sub>12</sub><sup>2+</sup> can be explained by the group scattering of the octahedral cluster, analogous to the typical low-resolution features of the Wilson plot for proteins. The Ta<sub>6</sub>Br<sub>12</sub><sup>2+</sup> cluster can therefore be expected to provide a significant phasing power at high resolution. This hypothesis has been tested using high-resolution data collected from crystals of four different Ta<sub>6</sub>Br<sub>12</sub><sup>2+</sup>-derivatized proteins.

Although at present the Ta<sub>6</sub>Br<sub>12</sub><sup>2+</sup> cluster compound is not produced commercially, it is possible that it will be available in the near future.

## 2. Materials and methods

### 2.1. Derivatization and data collection

The four test proteins, glucose isomerase (Carrell *et al.*, 1989), thaumatin (Ko *et al.*, 1994), thermolysin (Holmes & Matthews, 1982) and lysozyme (McPherson, 1982), were crystallized as described previously. The crystallization conditions for the four proteins are summarized in Table 1. Each crystal was derivatized by adding a 1 µl drop of a 6 mM solution of Ta<sub>6</sub>Br<sub>12</sub><sup>2+</sup> compound to a 5 µl drop of the mother liquor containing crystals. This procedure was repeated after 2 d, when the green color of the liquor faded and the crystals

acquired deep green coloration. Soaking times of longer than 4 d did not increase the amount of the anomalous signal in the data. All crystals were frozen at the beamline after being plunged into mother liquor containing approximately an additional 25% cryoprotectant (see Table 1) but lacking the tantalum cluster.

High-resolution X-ray data for all four test proteins were collected at the synchrotron beamline X9B, NSLS, Brookhaven National Laboratory using an ADSC Quantum 4 CCD detector and were reduced with the *HKL2000* suite (Otwinowski & Minor, 1997). Diffraction data for all crystals were collected using a

wavelength corresponding to the peak of the Ta fluorescence spectrum at 1.254 Å. A summary of the data collection and processing is given in Table 1.

In addition, a series of 1.8 Å resolution data sets were collected from the Ta<sub>6</sub>Br<sub>12</sub><sup>2+</sup>-derivatized crystal of glucose isomerase at ten different wavelengths, nine spanning the tantalum absorption edge in 2 eV intervals from 9876 to 9892 eV and one at the low-energy remote wavelength of 9681 eV. All of these data sets were of high quality, with *R*<sub>merge</sub> of about 3.5%, completeness above 98% and redundancy of 3.5. These ten sets were submitted to *XPREP* (Bruker Analytical X-ray Systems) for estimation of the *f'* and *f''* values at each wavelength on the basis of the anomalous signal contained in the measured intensities.

### 2.2. Phasing strategy

The positions of the anomalous scatterers (Ta atoms) were found by direct methods using *SHELXD* (Schneider & Sheldrick, 2002) on the basis of about 1500 of the largest normalized Bijvoet differences extracted from the original diffraction data by *XPREP*. The single-wavelength data and a number of highest *E*-map peak positions corresponding to Ta atoms were input into *SHARP* (de La Fortelle & Bricogne, 1997) and the resulting phases were forwarded to *SOLOMON* (Abrahams & Leslie, 1996) or *DM* (Cowtan & Zhang, 1999) for further modification by solvent flattening. In all cases the phase calculations with *SHARP* were carried out using the full resolution range of the data, except for glucose isomerase, where it was limited to 1.5 Å.

To obtain accurate phases for subsequent statistical comparisons, protein models taken from the PDB (Berman *et al.*, 2000; glucose isomerase, 1xib; thaumatin, 1thw; thermolysin, 8tln; lysozyme, 1lz8) were refined isotropically with *REFMAC* (Murshudov *et al.*, 1999) in combination with *wARP* (Lamzin & Wilson, 1997), except for glucose isomerase, which was finally refined anisotropically with *SHELXL*

(Sheldrick & Schneider, 1997), since these data extended to 1.3 Å resolution. The occupancies and *B* factors of the clusters and of some waters in all models were refined using *SHELXL*.

### 3. Results

#### 3.1. Crystal preparation and diffraction data

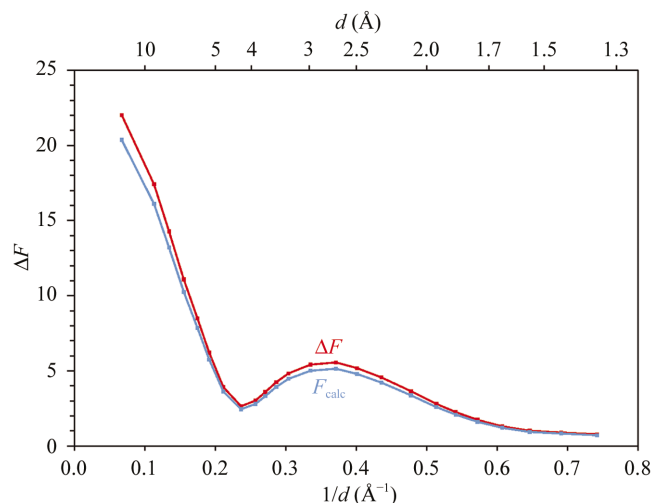
The four proteins were obtained from various crystallization conditions and were frozen in different cryosolutions, as shown in Table 1. All crystals were soaked in solutions containing about 2 mM of Ta<sub>6</sub>Br<sub>12</sub><sup>2+</sup> for 4 d, with a fresh drop of Ta<sub>6</sub>Br<sub>12</sub><sup>2+</sup> solution added again after 2 d. During the soaking procedure, all crystals gradually acquired a deep green color, in parallel with the disappearance of the color from the mother liquor, so that the progress of derivatization was easy to follow visually. The results of data collection proved that the relatively long soaking time did not impair the diffraction potential of the crystals. Moreover, the diffraction data obtained from the Ta<sub>6</sub>Br<sub>12</sub><sup>2+</sup>-derivatized crystal of glucose isomerase extended to 1.3 Å, a resolution that has never been achieved from fresh native crystals of this protein at the same beamline. In spite of rather high *R*<sub>merge</sub> in the highest resolution range, the *I*/*σ*(*I*) value shows that the data are significant to 1.3 Å resolution.

For all data sets the total rotation range was selected to ensure full completeness of the anomalous data, but no inverse-beam technique was used and no attempts were made to further increase the redundancy of measurements. The accuracy of intensity measurements was improved by the integration of the diffraction images in batches of three with concomitant post-refinement of the integration parameters (as implemented in the *HKL2000* program) and by the application of the pseudo-absorption correction in terms of the spherical harmonics in the scaling/merging procedure (again, an option of *HKL2000*).

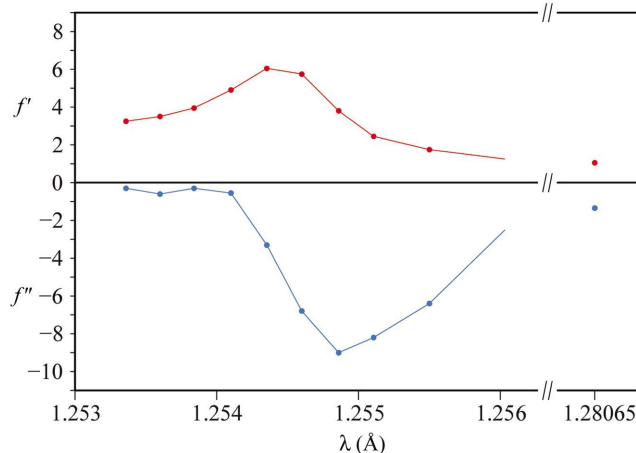
#### 3.2. Anomalous signal in the diffraction data

Fig. 1 shows the Bijvoet difference  $\Delta F^{\text{anom}}$  as a function of resolution for the glucose isomerase data. The distribution of structure amplitudes calculated from a single Ta<sub>6</sub> cluster positioned in a large unit cell is also plotted in the figure. The amount of the anomalous signal in the diffraction data closely parallels the cluster-group scattering behavior, diminishing at medium resolution and increasing at high resolution. The  $\Delta F^{\text{anom}}$  plots for the other data sets show the same characteristics.

The ( $\Delta F^{\text{anom}}/F$ ) Bijvoet ratio at the lowest resolution for thaumatin, thermolysin and lysozyme exceeds 6% and for glucose isomerase is 14%. At about 4.5 Å resolution, it diminishes to about 2.5% for all four crystals, but at about 2.5 Å rises to above 6% for thaumatin, thermolysin and lysozyme and to 10% for glucose isomerase. This is a significantly higher value than the 3% provided by one selenomethionine in 150 residues, usually accepted as sufficient for solving new structures by SeMet MAD phasing, despite the



**Figure 1**  
Bijvoet differences  $\Delta F^{\text{anom}}$  for the peak-wavelength data set of glucose isomerase as a function of resolution (red) and the structure amplitudes calculated from the single octahedron of Ta atoms (blue).



**Figure 2**  
Values of *f*' and *f*'' estimated by *XPREP* in ten Ta<sub>6</sub>Br<sub>12</sub><sup>2+</sup>-derivatized glucose isomerase data sets collected at wavelengths spanning the *L*<sub>III</sub> absorption edge of tantalum.

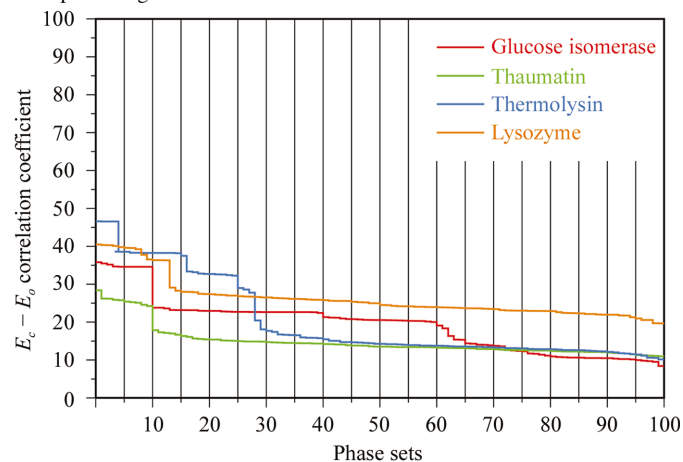


**Figure 3**  
Results of the identification of the anomalous Ta sites by *SHELXD* on the basis of the Bijvoet differences. The correlation coefficients (CC) between *E*<sub>o</sub> and *E*<sub>c</sub> for 100 phase sets are shown for glucose isomerase (red), thaumatin (green), thermolysin (blue) and lysozyme (brown). The phase sets with CC above 20% correspond to successful solutions of the anomalous scatterer substructure.

**Table 2**  
Phasing results.

| Protein  | Glucose isomerase   | Thaumatococcus                              | Thermolysin   | Lysozyme    |
|--|---|---|---|-------------|
| Protein size (kDa)                                       | 43  | 22  | 34  | 14          |
| Solvent content (%)                                      | 54  | 56  | 46  | 38          |
| No. of clusters  | 5   | 3   | 4   | 1           |
| Cluster occupancies ( <i>B</i> factors, Å <sup>2</sup> ) | 0.45 (36.3),<br>0.38 (18.3),<br>0.30 (41.0),<br>0.22 (34.3),<br>0.25 (30.2)†,<br>0.23 (34.8)† | 0.15 (26.1),<br>0.12 (32.7),<br>0.10 (32.1) | 0.18 (30.8),<br>0.07 (30.5),<br>0.07 (31.5),<br>0.05 (33.9) | 0.17 (26.1) |
| No. of clusters used for phasing                         | 2   | 2   | 1   | 1           |
| Mean FOM‡  |   |   |   |             |
| <i>SHARP</i>   | 0.48  | 0.30  | 0.36  | 0.42        |
| <i>SOLOMON</i>   | 0.92  | 0.83  | 0.89  | 0.89        |
| <i>DM</i>  | 0.80  | 0.73  | 0.75  | 0.79        |
| Phasing power‡   | 0.24  | 0.12  | 0.16  | 0.18        |
| Phase error (°)  |   |   |   |             |
| <i>SHARP</i>   | 60  | 77  | 62  | 68          |
| <i>SOLOMON</i>   | 25  | 36  | 32  | 57          |
| <i>DM</i>  | 34  | 57  | 51  | 51          |
| No. of residues built by <i>wARP</i> /total              | 369/388   | 200/207                                     | 309/316   | 120/129     |

† The occupancies and *B* factors of the disordered parts of the fifth cluster. ‡ From *SHARP*.

partial occupancy of the Ta<sub>6</sub>Br<sub>12</sub><sup>2+</sup> clusters in the investigated crystals.

*XPREP* analysis of the series of glucose isomerase data sets collected at different wavelengths reproduced the values of the dispersion corrections in almost perfect agreement with the expected characteristics of the Ta anomalous scattering (Fig. 2). The resonant white line was not highly pronounced, since the beam optics were adjusted for maximum intensity with a rather wide wavelength bandpass  $\delta\lambda/\lambda$ , suitable for a SAD but not for a MAD experiment. In the MAD experiment, the values of  $f'$  and  $f''$  are usually indirectly estimated from the fluorescence spectrum through the Kramer–Kronig transformation, e.g. with the program *CHOOCH* (Evans & Pettifer, 2001). These values can be refined in parallel with refinement of the anomalous scatterer parameters and phase evaluation. However, in such a refinement procedure the values of  $f'$  and  $f''$  are correlated with other parameters, such as the anomalous scatterer occupancies and the overall scale factor. Most of the phasing programs treat the  $f'$  and  $f''$  values as fixed known parameters. As shown in Fig. 2, good estimates of these values can be extracted directly from the diffraction data if measurements at more than one wavelength are available. However, it is not possible to extract these values from the single-wavelength data set. The ten-wavelength glucose isomerase data sets were collected in order to estimate the correct values of  $f'$  and  $f''$  for Ta at the peak wavelength at which all other data were measured.

### 3.3. Identification of the anomalous sites and SAD phasing

The sites of anomalously scattering Ta atoms were identified by direct methods on the basis of the Bijvoet differences. For all data sets the 100 phase trials from *SHELXD* contained a number of successful solutions, characterized by a  $E_c - E_o$  correlation coefficient higher than 25% (Fig. 3). The correct-

ness of the solutions could be corroborated by analysis of the *SHELXD* 'crossword table', which lists distances between all pairs of the identified anomalous scatterer sites. It was easy to identify peaks belonging to individual clusters at mutual distances of 2.7 Å. Because of the partial occupancies of the clusters, there was a little contrast in the peak heights between the correct and spurious sites; the tantalum sites were accepted for the subsequent *SHARP* phasing on the basis of their classification into the individual clusters as revealed by the interpeak distances. Two complete clusters could be convincingly identified for glucose isomerase and thaumatococcus and one complete cluster for thermolysin and lysozyme. *A posteriori* comparison with peaks in the anomalous difference maps calculated with refined phases showed

that several more peaks in the *SHELXD* lists corresponded to the correct Ta positions, particularly for glucose isomerase, thaumatococcus and thermolysin. As stated previously, only those Ta sites which were identified as complete octahedral clusters were used for phasing, in spite of the presence of more *SHELXD* peaks which were later confirmed in the anomalous difference map as correct Ta positions (see also Table 2).

The Ta sites were input to *SHARP* for evaluation of phases on the basis of the single-wavelength data. Phase modification by solvent flattening was performed by *SOLOMON* (within the *SHARP* interface) and in parallel by *DM*. The regions of the resulting maps are presented in Figs. 4(a)–4(d). These two procedures gave comparable results (Table 2), except for thaumatococcus, where *SOLOMON* gave a readily interpretable map in contrast to *DM*, and for lysozyme, where *DM* produced a map of higher quality than *SOLOMON*. As a result of rather weak incorporation (occupancy below 0.15) of Ta<sub>6</sub>Br<sub>12</sub><sup>2+</sup>, the starting phase set for thaumatococcus had the largest phase error (77°); however, because the crystals of thaumatococcus are characterized by the highest solvent content (56%) of all crystals tested, the density modification implemented in *SOLOMON* was able to refine even such inaccurate phases. In contrast, for lysozyme, characterized by the lowest solvent content (38%), the density modification was least successful and only the *DM* map could be automatically traced by *wARP*. The average phase differences between the final refined phases and the initial *SHARP* phase estimations as well as phases after density modification are presented in Fig. 5 as a function of resolution.

The crystal solvent content is also important for the success of the Ta<sub>6</sub>Br<sub>12</sub><sup>2+</sup> phasing in another context. An attempt to derivatize xylanase crystals using Ta<sub>6</sub>Br<sub>12</sub><sup>2+</sup> was unsuccessful; these crystals did not acquire the green color during several days of soaking. They contained only 38% solvent and the tight packing of protein molecules and the narrow solvent

channels evidently precluded any significant penetration of crystals by the bulky  $\text{Ta}_6\text{Br}_{12}^{2+}$  clusters. The crystals of lysozyme contained the same amount of solvent as xylanase, but evidently their intermolecular solvent channels allowed some diffusion of  $\text{Ta}_6\text{Br}_{12}^{2+}$  into only one weak site.

### 3.4. $\text{Ta}_6\text{Br}_{12}^{2+}$ cluster sites

The  $\text{Ta}_6\text{Br}_{12}^{2+}$ -cluster sites in the four structures were initially located by a direct-methods solution of the anomalous scatterer substructures using the *SHELXD* program run against the Bijvoet differences. The anomalous difference map, calculated with the phases corresponding to the refined models, confirmed the correctness of the initial sites and identified additional sites with lower occupancies in glucose isomerase, thaumatin and thermolysin. Of the total of 13  $\text{Ta}_6\text{Br}_{12}^{2+}$  clusters in the four structures, only one displays

double orientation; in the remaining 12 sites the  $\text{Ta}_6\text{Br}_{12}^{2+}$  ions have well defined single orientations. One of the clusters located around the molecule of glucose isomerase is shown in Fig. 6. At the tantalum peak wavelength of 1.254 Å, Br atoms do not display any significant anomalous scattering effect. Since the  $\text{Ta}_6\text{Br}_{12}^{2+}$  clusters are rigid and the Br positions are at all 12 edges of the octahedron formed by the Ta atoms, in the subsequent modeling the Br atoms were located geometrically and refined with the appropriate distance restraints. Most of the Br atoms had corresponding density in the  $2F_o - F_c$  maps.

The cluster sites are located within the solvent region near the surface of the protein molecules, but there is no clear preference in their binding for specific protein functions. There are no distances between the cluster (Ta or Br) and protein atoms of shorter than 4.1 Å. Several clusters have charged protein groups in their vicinity, both positively (side chains of Arg or Lys) and negatively (Glu or Asp) charged.

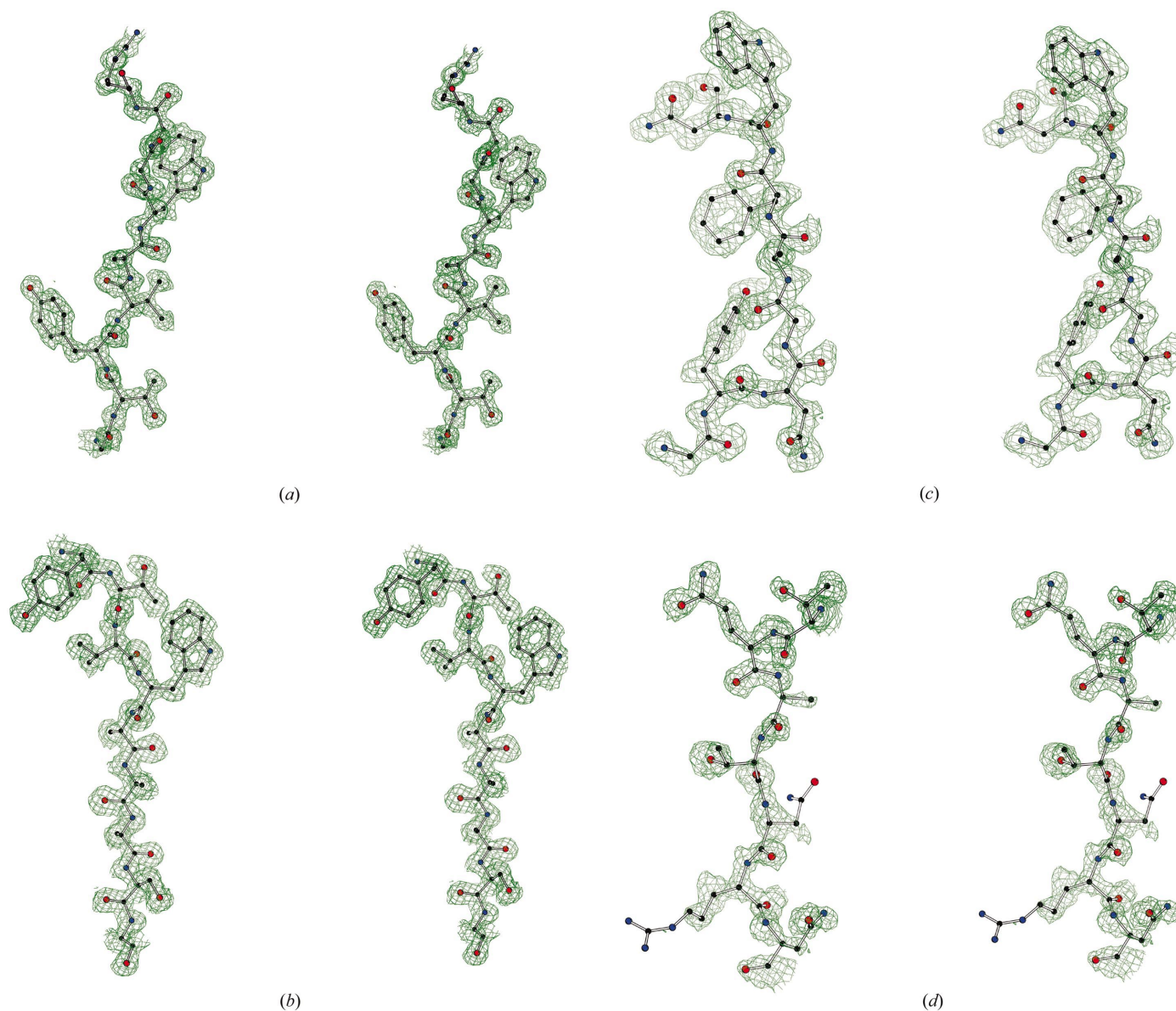


**Figure 4** Stereoview of the experimental solvent-flattened maps plotted at the  $1\sigma$  level for (a) glucose isomerase, (b) thaumatin, (c) thermolysin and (d) lysozyme.

There is no indication for the coordination of the protein carboxyl groups as apical ligands of the Ta atoms. Such a coordination might be expected as the Ta cluster ion in aqueous solution coordinates six water molecules as apical Ta-atom ligands and should in fact be represented by the formula  $\text{Ta}_6\text{Br}_{12}(\text{H}_2\text{O})_6^{2+}$  (Knäblein *et al.*, 1997).

The occupancies and  $B$  factors of the cluster sites were estimated by *SHELXL* refinement and the resulting values are given in Table 2. These values are approximate, since at 1.5 Å resolution the site occupancies are highly correlated with  $B$  factors and, in addition, the cluster sites superimpose with partially occupied water molecules which were not modeled. However, only in glucose isomerase do the cluster

site occupancies exceed 0.2. In the crystals of thaumatin, which like glucose isomerase has a solvent content of about 55%, the cluster occupancy is below 0.15. In thermolysin and lysozyme, which are tightly packed, the cluster occupancies are also low. Glucose isomerase is the largest of the four tested proteins, which may explain the larger number of  $\text{Ta}_6\text{Br}_{12}$  sites around its molecule.

In spite of the low occupancies of their sites, the anomalous signal of the  $\text{Ta}_6\text{Br}_{12}$  clusters was sufficient for a successful SAD phasing of all four structures. However, a single  $\text{Ta}_6\text{Br}_{12}$  cluster with occupancy 0.15 at high resolution provides the anomalous scattering signal equivalent to one fully occupied Ta atom: about six electron units, according to Fig. 1. At low resolution, when the individual Ta atoms are not resolved, the anomalous signal is much higher, since the clusters scatter as super-atoms.

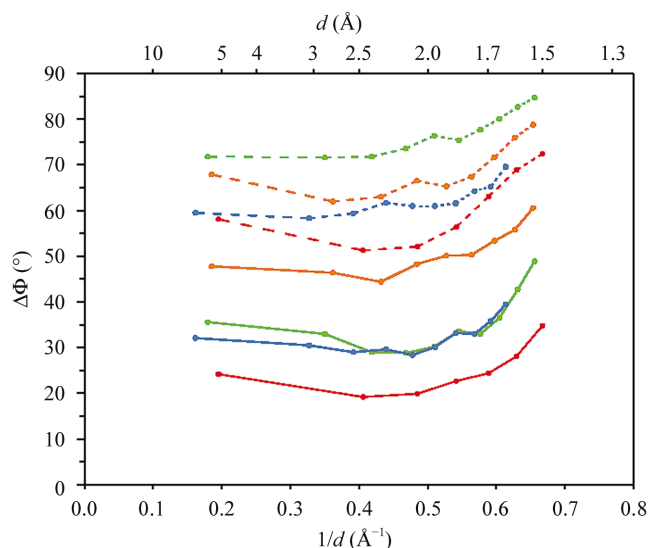


**Figure 5**  
The average phase differences between the refined model phases and the phases obtained after their initial estimation by *SHARP* (dashed lines) and after density modification (solid lines). The lines are colored as in Fig. 3.

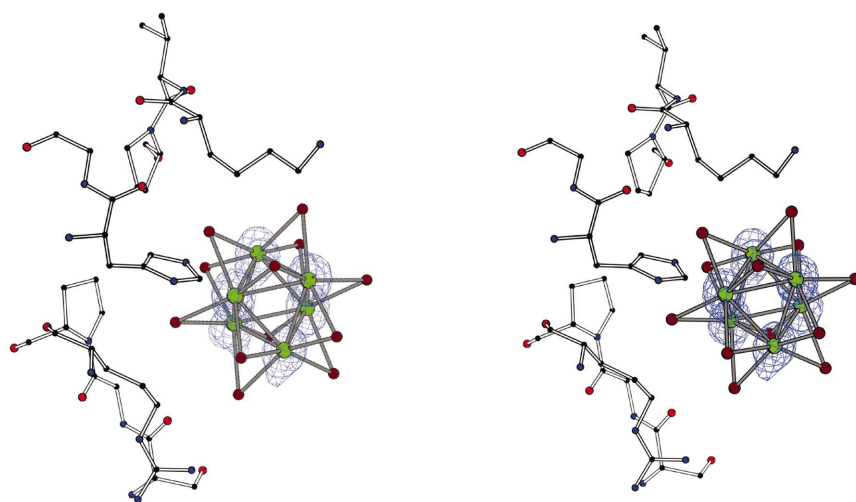


**Figure 6**  
One of the  $\text{Ta}_6\text{Br}_{12}$ -cluster sites positioned in the crystal structure of glucose isomerase with anomalous difference density at the  $5\sigma$  level. The occupancy of this cluster is 0.38 and the average  $B$  factor of the Ta atoms is  $18.3 \text{ \AA}^2$ .

#### 4. Conclusions

The  $\text{Ta}_6\text{Br}_{12}^{2+}$ -cluster compound derivatizes protein crystals in a mild fashion, possibly even stabilizing the crystalline order, which may sometimes lead to the improved diffraction of crystals soaked in this reagent. The additional benefit is provided by its deep green color, which is absorbed by crystals, so that the progress of derivatization is easy to follow. The cluster ions usually bind with partial occupancies, but they are in general not spherically disordered; if the resolution of the diffraction data extends beyond 3 Å then it is possible to resolve a majority of the individual Ta-atom sites.

The X-ray absorption edge of tantalum lies at a wavelength of 1.254 Å, which is easily accessible on almost all tunable synchrotron beamlines. The Ta fluorescence spectrum displays a very pronounced white line. Even when partially incorporated, the  $\text{Ta}_6\text{Br}_{12}^{2+}$ -cluster ions, with their six Ta atoms, provide a strong phasing power at this wavelength. Owing to the octahedral shape of  $\text{Ta}_6\text{Br}_{12}^{2+}$ , its anomalous scattering effect is very large at a resolution lower than 5 Å, diminishes at about 4 Å and becomes significant again at a resolution higher than 3 Å. At high resolution the anomalous scattering signal of Ta can be successfully used in the SAD approach and, in combination with the dispersive differences between data collected at different wavelengths, may provide even more powerful phasing in the MAD mode.

We thank Gunther Schneider for his kind gift of the  $\text{Ta}_6\text{Br}_{12}^{2+}$  compound.

#### References

- Abrahams, J. P. & Leslie, A. G. W. (1996). *Acta Cryst.* **D52**, 30–42.
- Ban, N., Nissen, P., Hansen, J., Moore, P. B. & Steitz, T. A. (2000). *Science*, **289**, 905–920.
- Berman, H. M., Westbrook, J., Feng, Z., Gilliland, G., Bhat, T. N., Weissig, H., Shindyalov, I. N. &

- Bourne, P. E. (2000). *Nucleic Acids Res.* **28**, 235–242.
- Carrell, H. L., Glusker, J. P., Burger, V., Manfre, F., Tritsch, D. & Biellmann, J. F. (1989). *Proc. Natl Acad. Sci. USA*, **86**, 4440–4444.
- Cowtan, K. D. & Zhang, K. Y. J. (1999). *Prog. Biophys. Mol. Biol.* **72**, 245–270.
- Dauter, Z., Dauter, M. & Dodson, E. J. (2002). *Acta Cryst.* **D58**, 494–506.
- Evans, G. & Pettifer, R. F. (2001). *J. Appl. Cryst.* **34**, 82–86.
- Gomis-Rüth, F. X. & Coll, M. (2001). *Acta Cryst.* **D57**, 800–805.
- Hendrickson, W. A. & Ogata, C. M. (1997). *Methods Enzymol.* **276**, 494–523.
- Holmes, M. A. & Matthews, B. W. (1982). *J. Mol. Biol.* **160**, 623–639.
- Knäblein, J., Neufeind, T., Schneider, F., Bergner, A., Messerschmidt, A., Löwe, J., Steipe, B. & Huber, R. (1997). *J. Mol. Biol.* **270**, 1–7.
- Ko, T. P., Day, J., Greenwood, A. & McPherson, A. (1994). *Acta Cryst.* **D50**, 813–825.
- La Fortelle, E. de & Bricogne, G. (1997). *Methods Enzymol.* **276**, 472–494.
- Lamzin, V. S. & Wilson, K. S. (1997). *Methods Enzymol.* **277**, 269–305.
- Lindqvist, Y., Schneider, G., Ermler, U. & Sundstöm, M. (1992). *EMBO J.* **11**, 2373–2379.
- McPherson, A. Jr (1982). *The Preparation and Analysis of Protein Crystals*. New York: John Wiley.
- Murshudov, G. N., Vagin, A. A., Lebedev, A., Wilson, K. S. & Dodson, E. J. (1999). *Acta Cryst.* **D55**, 247–255.
- Otwinowski, Z. & Minor, W. (1997). *Methods Enzymol.* **276**, 307–326.
- Rice, L. M., Earnest, T. N. & Brunger, A. T. (2000). *Acta Cryst.* **D56**, 1413–1420.
- Smith, J. L. & Hendrickson, W. A. (2001). *International Tables for Crystallography*, Vol. F, edited by M. G. Rossmann & E. Arnold, pp. 299–303. Dordrecht: Kluwer Academic Publishers.
- Schneider, F., Löwe, J., Huber, R., Schindelin, H., Kisker, C. & Knäblein, J. (1996). *J. Mol. Biol.* **263**, 53–69.
- Schneider, G. & Lindqvist, Y. (1994). *Acta Cryst.* **D50**, 186–191.
- Schneider, T. R. & Sheldrick, G. M. (2002). *Acta Cryst.* **D58**, 1772–1779.
- Sheldrick, G. M. & Schneider, T. R. (1997). *Methods Enzymol.* **277**, 319–343.
- Thygesen, J., Weinstein, S., Franceschi, F. & Yonath, A. (1996). *Structure*, **4**, 513–518.